

Sol-gel synthesis, characterization and photocatalytic activity of mixed oxide ZnO-Fe₂O₃

Aracely Hernández · Lourdes Maya · Enrique Sánchez-Mora · Eduardo M. Sánchez

Received: 2 August 2006 / Accepted: 5 December 2006 / Published online: 1 February 2007
© Springer Science + Business Media, LLC 2007

Abstract Synthesis by sol-gel method of mixed semiconductor ZnO-Fe₂O₃ was carried out using inorganic salts as precursors. The powders were synthesized at different pH (neutral and basic) in order to study its influence on the properties of the catalysts. These materials were characterized by thermal analysis TGA-DTA, X-ray Diffraction, FTIR spectroscopy, scanning electron microscopy and X-ray energy dispersive spectroscopy. The specific surface area of the solids was calculated from nitrogen adsorption isotherms by BET method. The band gap energy (E_g) of the catalysts was obtained from its UV-Vis spectra (diffuse reflectance) when the crystalline phase was formed under thermal treatment at 350°C by 3 h. The incorporation of Fe₂O₃ to ZnO semiconductor gives as a result a lower E_g value for zinc oxide. Catalytic activity of the materials was evaluated using as test reaction the photocatalytic degradation of potassium cyanide in aqueous dissolution. The catalyst ZnO-Fe₂O₃ synthesized at pH 7 turned out to be superior than sol-gel and commercial ZnO under similar conditions.

Keywords Sol-gel · Zinc oxide · Iron oxide · Photocatalysis · Cyanides

Introduction

Photocatalytic oxidation using a semiconductor oxide, has been developed extensively for the complete oxidation of low levels of organic and inorganic compounds on water [1–4]. In heterogeneous photocatalysis, dispersed solid particles absorb larger fractions of the UV spectrum efficiently and generate chemical oxidants in situ from dissolved oxygen or water [5]. Whenever different semiconductor materials have been tested under comparable conditions for the degradation of the same compounds, TiO₂ has generally been demonstrated to be the most active. In spite of this, the active phase, anatase, do not absorb significantly over 360 nm, then the activity decreases when only visible light is used. The efforts to achieve a more efficient photocatalytic process, are in direction to improve the TiO₂ response, or to look for new semiconductor materials with adequate electronic properties.

Many research works have focused on mixed oxide semiconductors due to an efficient charge separation can be obtained by coupling two semiconductor particles with different energy levels [6–9]. The improvement in efficiency of photocatalytic reactions is explained as result of a vectorial transfer of photo-generated electrons and holes from a semiconductor to another [10, 11]. ZnO has electronic properties and band gap energy similar to TiO₂ and it has been reported sometimes to be more efficient than TiO₂ for the photooxidation of phenol and nitrophenols [12, 13]. However, some combinations of ZnO with Fe₂O₃, TiO₂ or WO₃ have been investigated in order to enhance its photocatalytic activity on organic compounds photodegradation. In other researches, Fe₂O₃ has been used as a coupling semiconductor with TiO₂ to extend its optical absorption edge into the visible light region [14–18].

A. Hernández (✉) · L. Maya · E. M. Sánchez
Fac. de Ciencias Químicas, Universidad Autónoma
de Nuevo León,
San Nicolás de los Garza, N.L. México
e-mail: ahernandez@fcq.uanl.mx

E. Sánchez-Mora
Instituto de Física, Universidad Autónoma de Puebla,
Apdo. postal 1651, Puebla, Pue. 72000, México

On the other hand, photocatalytic activity of a semiconductor depends on its preparation method since this affects the physicochemical properties of the solids. Sol-gel process is a powerful method for tailoring transition metal oxides to fit particular applications. Alcoxide sol-gel route is widely accepted for synthesizing advanced materials with tailored properties; however, for large-scale application it is somehow expensive. Making gels in a simple and inexpensive way is by means of inorganic sol-gel route, using as a precursor an aqueous or alcoholic mixture of metal organic or inorganic salts. The main advantage of the sol-gel method is the molecular level homogeneous mixing of transition-metal cation which enhances the formation of polycrystalline particles with special properties [19]. In this work, we reported the synthesis and characterization of mixed photocatalyst ZnO-Fe₂O₃ (1.0 wt.%) by sol-gel method. We studied the activity of the catalysts using as a test reaction the photocatalytic degradation of cyanide in aqueous dissolution. Up to now, photocatalytic activity of this coupled system has not been studied on degradation of an inorganic toxic substance such as potassium cyanide.

Experimental

Synthesis

Two synthesis of mixed oxide ZnO-Fe₂O₃ were carried out at different pH conditions: neutral at pH 7 and basic at pH 9. A quantity of (0.09 moles) of Zinc acetate Zn(CH₃COO)₂*2H₂O (Baker 98%) and 1.0 wt% of FeCl₃*6H₂O (PROQUIM 99.8%) were dissolved in 200 ml of water. An aqueous solution of NH₄OH (PROQUIM 99.8%) was added under continuous stirring to give the corresponding pH in each synthesis. The reaction mixture was maintained at room temperature until a gel was formed; once the colloid was observed, it was aged for 24 h which was dried in the oven at 80°C (fresh sample) and then calcined in an electrical furnace at 350°C for 3 h. For comparative purpose, at similar conditions, we also prepared pure zinc oxide at pH 9.

Characterization

Thermal analysis

The DTA and TGA curves of the fresh sample mixed oxides were recorded in a TA-Instruments SDT-2960 thermal analyzer in argon atmosphere, using a heating rate of 10°C min⁻¹ and the reference substance was alumina.

FTIR spectroscopy

The hydroxy groups on the catalysts were studied by infrared absorption spectroscopy using a Perkin Elmer FT-IR Spectrometer Paragon 1000 PC. The samples were mixed with KBr and pressed under 7 tons to obtain a transparent pellet.

X-ray diffraction technique

The samples were analyzed by a Siemens D-5000 diffractometer with Cu-K α radiation ($\lambda = 1.5418 \text{ \AA}$). The reflection intensities were measured by step scanning in the 2θ range between 10° and 85°, with a step size of 0.05°.

UV-Vis spectroscopy

The UV-Vis absorption spectra of the samples were obtained by diffuse reflectance studies using a Perkin Elmer spectrophotometer model Lambda 12 coupled to an integration Labsphere RSA-PE-20. A Spectralon standard USRS-99010 with 100% reflectance was used as reference.

Specific surface area

Nitrogen adsorption isotherms of the samples were measured using an Autosorb-1 instrument (Quantachrome Corporation). The surface area was calculated by the BET equation.

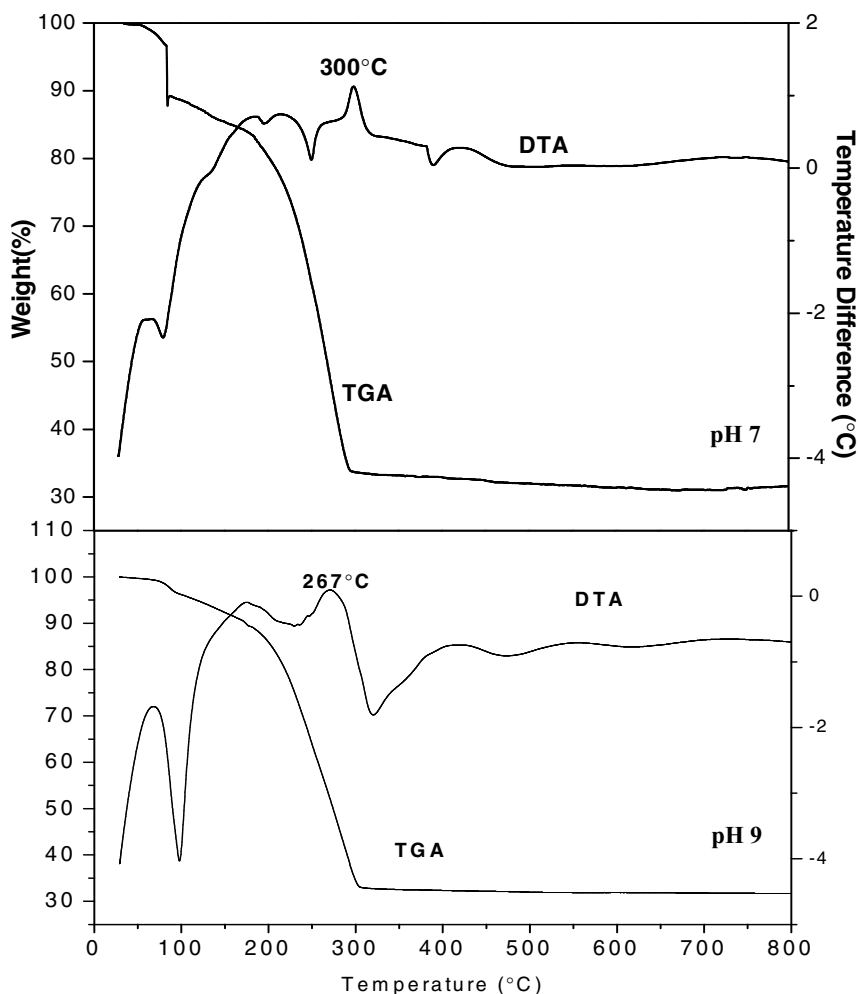
SEM-EDS

The materials obtained were analyzed by SEM and X-ray energy dispersive spectroscopy using a JEOL JSM-5400 LV Scanning electron microscope equipped with a Noran Voyager EDS system.

Photocatalytic activity

Photocatalytic experiments were carried out at room temperature. A quantity of 150 mg of catalyst was added to a flask containing 250 ml of an aqueous solution of potassium cyanide at $3.33 \times 10^{-4} \text{ M}$. Under stirring, the solution was irradiated in a closed box with a UV lamp Spectroline XX-15N which emits radiation at 365 nm and its intensity is of 2000 $\mu\text{W}/\text{cm}^2$. The light intensity received by the vessel was measured with a Mannix UV-340 UV Light Meter 290–390 nm (UVA-UVB). The reaction rate was followed by taking aliquots every 20 min and then analyzed by potentiometric method using an ISE Meter Orion (Model 720A) with an ion selective cyanide electrode. A certificated potassium cyanide standard (Ricca Chemical Co.) was used to prepare the calibration curve.

Fig. 1 TGA and DTA curves of mixed oxide ZnO-Fe₂O₃ fresh sample

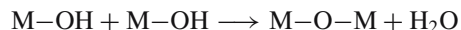


Results and discussion

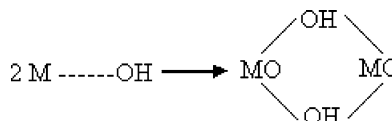
Thermal analysis

In Fig. 1, the thermal analysis curves of the heated fresh samples prepared at pH 7 and 9 are showed. TGA curves are very similar where a progressive 65% weight variation is observed from initial temperature until 300°C. The first weight loss (15%) which is observed from room temperature to 200°C, is associated with the loss of water physically absorbed into the solid. The posterior weight loss zone, present from 200 to 300°C, can be attributed to acetate residual groups desorption. Significant differences between DTA curves of the samples synthesized at basic and intermediate pH are observed. The large endothermic peak at 100°C, on the sample obtained at pH 9, can be explained according to the condensation mechanism on the sol-gel process from inorganic precursors. At basic medium, for lower cation charge ($z = 2, 3$), the hydroxide is the common ligand to the central transition metal ion. M–OH bonds are formed and water molecules

formation predominates [20]. Then, oxolation in the condensation process is the present mechanism in the synthesis at pH 9 and it leads to the formation of oxo bridges:

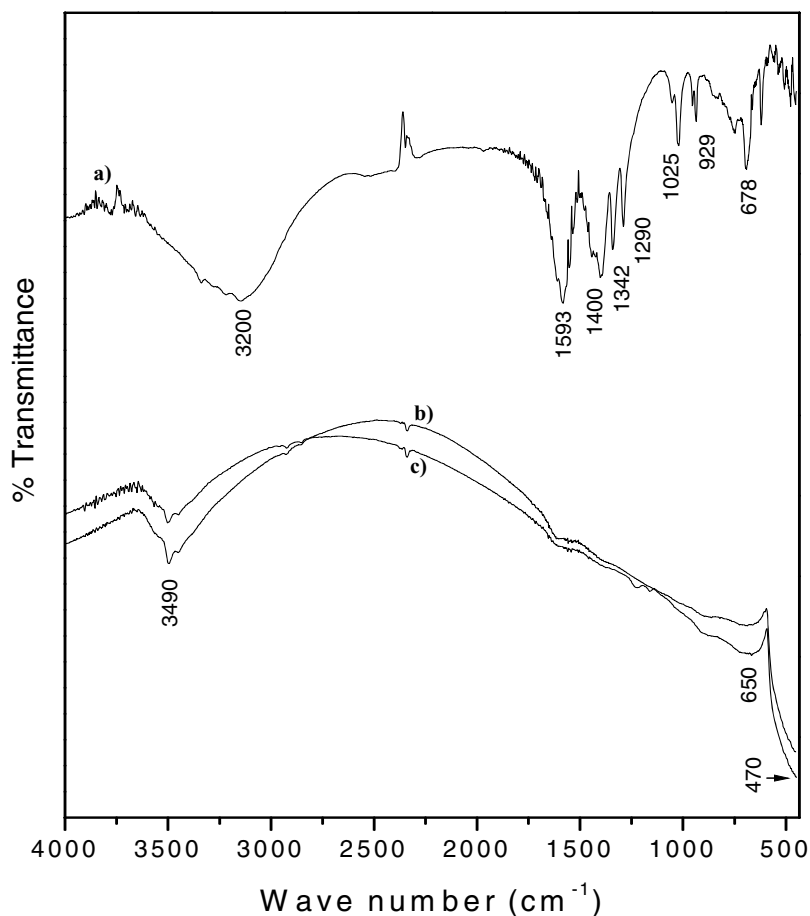


Hence, the fresh sample has a large quantity of water occluded into the gel that needs more energy to be desorbed during thermal treatment. DTA curve of the gel obtained at pH 7 exhibits a small endothermic peak at 100°C which is indicative of easily surface water evaporation. No water molecules formation is present at this neutral pH because hydroxo bridges are formed due to the olation mechanism that is favored on the condensation step at neutral pH [21].



At the same time, we observed an endothermic peak at approximately 400°C which can be attributed to the

Fig. 2 FTIR spectra of (a) ZnO-Fe₂O₃ fresh sample, (b) ZnO-Fe₂O₃ pH 7 at 350°C and (c) ZnO-Fe₂O₃ pH 9 at 350°C



dehydroxilation process [22] evidenced by the small weight loss in the TGA curve at this temperature. This same behavior in the DTA curve (Fig. 1) of the sample at pH 9 is exhibited at 320°C, which means that hydroxyl groups are weakly tied to the zinc oxide network when the solid is obtained at this pH.

On the other hand, the exothermic peak, which indicates a crystallization process, is observed also at a lower temperature (267°C) in the synthesis at pH 9 than synthesis at pH 7 (300°C). In the fresh sample, the mixed oxide is amorphous; then, we can assume that at basic pH the formation of smaller particles is favored, which permits the production of a crystalline arrangement at a low temperature. This is in agreement with previous reports on sol-gel synthesis at different pH, where the crystalline compound is formed at a low temperature when the hydrolysis reaction is carried out at basic conditions [23].

Infrared spectroscopy

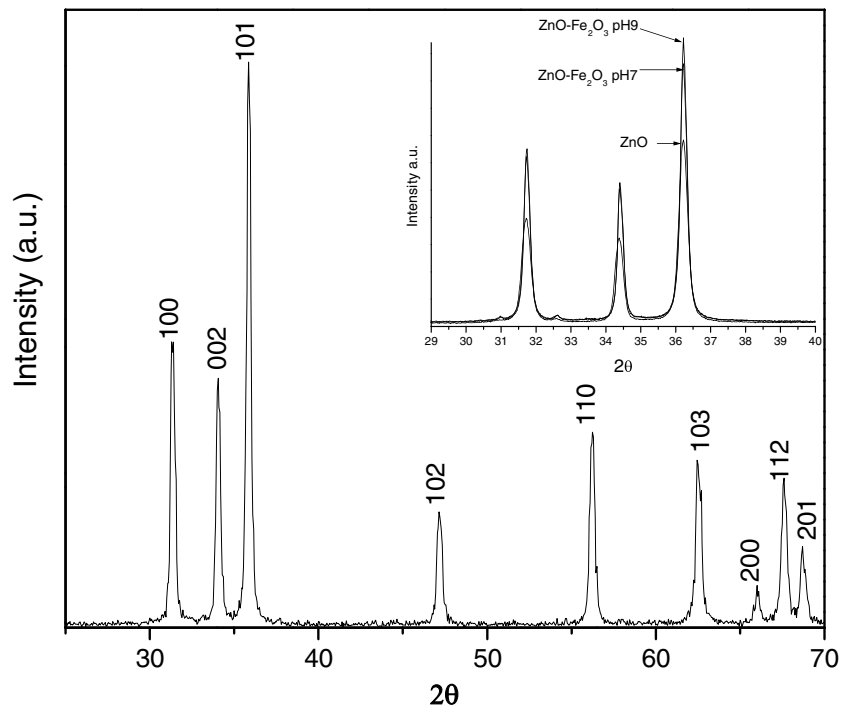
FTIR spectroscopy studies of the sol-gel mixed oxide show that fresh samples spectra (Fig. 2), exhibit a wide absorption band at 3200 cm⁻¹ which is assigned to the stretching vibrations of hydroxy groups from water molecules occluded in the solid. The bands located at 1593 and 1430 cm⁻¹ cor-

respond to symmetric C=O and C-O stretching vibrations due to the retention in the gel of acetate residuals groups; at the same time, we can observe a bending band at 678 cm⁻¹ which is characteristic of the O-CO groups frequencies. At 1025 cm⁻¹ rocking vibrations of CH₃ groups are shown, meanwhile, the bands located at 1400 and 1342 cm⁻¹ correspond to symmetric and asymmetric C-H bending vibrations [24]. Such bands disappeared once the fresh sample was thermally treated. Both fresh samples spectra (pH 7 and pH 9) showed similar absorption bands. The spectra of the samples annealed at 350°C shows that the OH bands diminish and they shift to higher energy values at 3490 cm⁻¹ which indicates that hydroxy groups remaining are chemically bonded to the oxide network [23]. Such band is less intense in the sample synthesized at pH 9. The wide absorption band observed in the low energy region is formed by the stretching vibrations modes of Zn-O and Fe-O bonds (650 and 470 cm⁻¹) [25, 26].

Powder X-ray diffraction

X-ray diffraction pattern of the mixed oxide synthesized at pH 7 and annealed at 350°C, is shown on Fig. 3. It can be observed the corresponding peaks to the position of the ZnO

Fig. 3 X-ray diffraction pattern of the mixed oxide ZnO-Fe₂O₃ synthesized at pH 7



reflections related to crystalline hexagonal phase (zincite) [27]. The Fe₂O₃ reflections were not observed since X-ray powder diffraction technique is unable to detect lower percentages than 5% of an impurity or crystalline phase [28], a similar diffraction pattern was obtained for the sample prepared at pH 9. These results are in agreement with Sakthivel and co-workers research in relation to the study of various semiconductors deposited on ZnO [29], however, the samples exhibit a slightly orange color and the content of iron in the mixed oxide was confirmed by EDS analysis.

When the diffraction pattern of ZnO sol-gel was compared with those of ZnO-Fe₂O₃ at pH 7 and ZnO-Fe₂O₃ at pH 9 (insert in the Fig. 3), it was not observed a change on the main reflections associated to the ZnO structure, which could indicate that doping agent is dispersed on the ZnO surface. For this comparative study, the XRD pattern of each sample was slowly recorded using KCl as internal standard.

Band gap energy

The UV-Vis absorption spectra of the samples heated at 350°C are compared with commercial ZnO and prepared

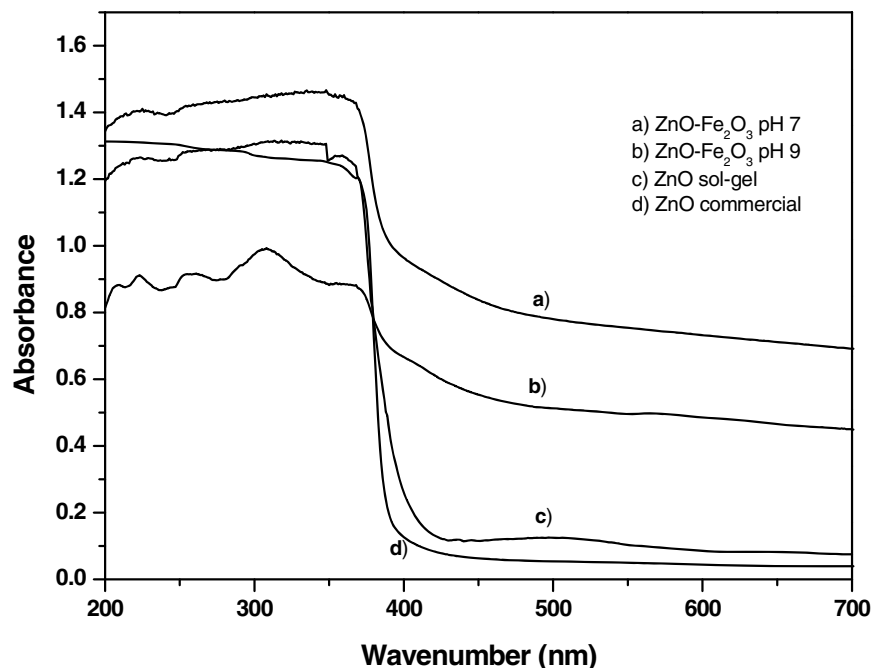
ZnO spectra in Fig. 4. We can see for commercial and sol-gel ZnO samples, a single intense absorption edge at about 390 and 420 nm respectively, which corresponds to a charge-transfer process from the valence band to the conduction band of semiconductor oxide [29]. Meanwhile, we can observe two adsorption regions on mixed oxide ZnO-Fe₂O₃ synthesized at pH 7 spectra. The first one is observed at low energy in the visible region, between 390 and 480 nm, which is ascribed to the small Fe₂O₃ content in the mixed oxide. The second absorption edge is assigned to the absorption of the ZnO which presents a displacement towards higher wavelength values (435 nm) on respect to commercial zinc oxide and similar to ZnO prepared by sol-gel. In the case of the ZnO-Fe₂O₃ synthesized at pH 9 we can see an absorption edge at 500 nm with a maximum at 370 nm which it is attributed at the major content of iron oxide.

The values of the band gap energy of the zinc oxide powders and mixed oxide samples annealed at 350°C, were calculated from the equation $\alpha(h\nu) = A(h\nu - E_g)^{m/2}$, whereby α is the absorption coefficient, $h\nu$ is the photon energy and $m = 1$ represent a direct transition between bands (valence band and conduction band). From the UV-Vis spectra, E_g

Table 1 Band gap energy values and elemental analysis of mixed oxide and pure Zinc oxide catalysts

Sample	E_g (eV)	Atomic percentage			Elemental percentage		
		Zn	O	Fe	Zn	O	Fe
ZnO-Fe ₂ O ₃ pH 7	2.84	45.54	54.0	0.46	76.99	22.35	0.66
ZnO-Fe ₂ O ₃ pH 9	2.66	45.83	53.19	0.98	76.79	21.81	1.4
ZnO sol-gel	3.07	48.87	51.13	–	79.6	20.4	–
Commercial ZnO	3.17	–	–	–	–	–	–

Fig. 4 UV-Vis absorption spectra of different zinc oxide catalysts



was calculated by extrapolating a straight line from the absorption curve to the abscissa axis. When α is zero, then $E_g = h\nu$ [30, 31]. From the slopes observed on the UV-Vis spectra of each sample, we calculate E_g values reported in Table 1. These values are closer to those reported for ZnO in the literature [32], however, in mixed oxide this band gap value is lower than pure zinc oxide.

When samples are synthesized at pH 7, the E_g values are higher than those of the samples prepared at pH 9. The hydrolysis reaction at pH 7 is faster and almost complete for zinc acetate, however for FeCl_3 does not totally occur. Therefore, according to the EDS studies, less Fe_2O_3 is incorporated to the mixed oxide, consequently the shift absorption band toward visible region edge is lower and the E_g values increase. In the synthesis at pH 9, FeCl_3 is totally hydrolyzed and the iron incorporation is complete. Therefore, at higher iron content in mixed oxide, the absorption of light in the visible region by the ZnO, increases which gives as a result lower E_g values. This is in agreement with previous works on mixed semiconductor powders [16, 17]. However, the activity of the mixed semiconductor depends of an optimum content of iron oxide [29] and its surface characteristics.

SEM and X-ray energy dispersive spectroscopy

In Fig. 5 SEM images of the surface morphology of mixed oxide thermally treated are shown. It can be observed that both samples consist of crystallite aggregates with differ-

ent shape and size of the particles. The sample obtained at pH 7 (Fig. 5(a)) exhibits secondary particles with combination of linear and irregular shape; the size of the particles is greater than 100 nm. However, the sample synthesized at pH9 exhibits spherical particles with a diameter size averaging 100 nm together to form dense agglomerates. It has been reported that a basic pH in the sol-gel synthesis yields more highly branched clusters, otherwise at a low pH primarily linear or randomly branched polymers are achieved [19], then at pH 7 the linear shape of the particles produces a less dense material which could facilitate the transport of reactants and products through the catalysts.

From the EDS spectra of the mixed semiconductors, we obtained the elemental analysis of each sample showed in Table 1. From these results we confirm that the synthesis conditions cause changes on the sol-gel process. During the hydrolysis mechanism that takes place on the sol-gel method, different kind of ligands in the medium are formed due to the nucleophilic water attack. The type of ligand produced depends on the cation charge and the solution pH, hence the characteristics of the synthesized powders are different. As we pointed out before, at pH 9 the iron incorporation is complete [20] since at this pH the hydrolysis process is slower and the polymerization is catalyzed by the basic medium which permit the total formation of iron oxide, otherwise at pH 7, the incomplete hydrolysis originates residual molecules of the iron precursor and therefore less iron is incorporated.

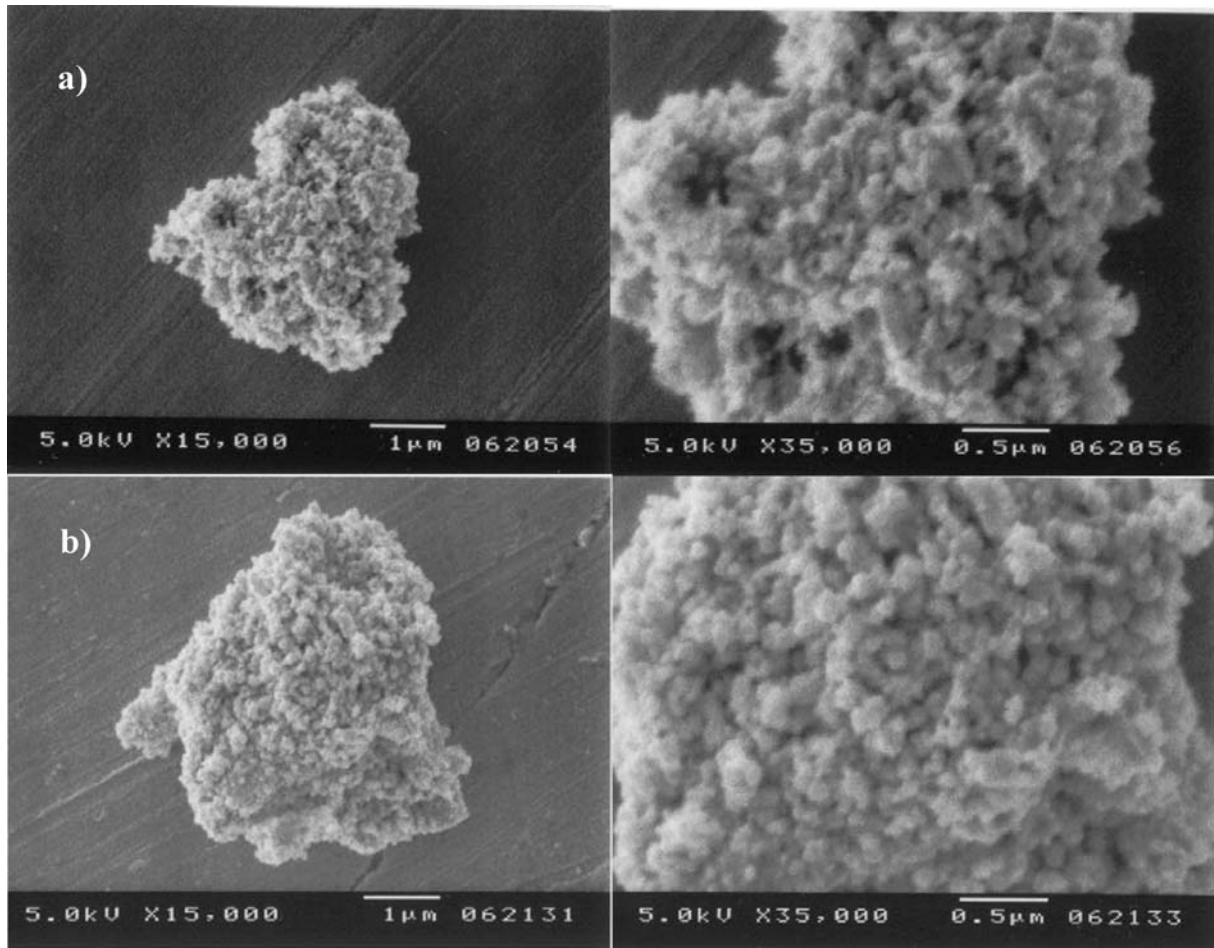


Fig. 5 SEM images of (a) ZnO-Fe₂O₃ pH 7 at 350°C and (b) ZnO-Fe₂O₃ pH 9 at 350°C

Fig. 6 Potassium cyanide decomposition on mixed oxide ZnO-Fe₂O₃ and pure ZnO

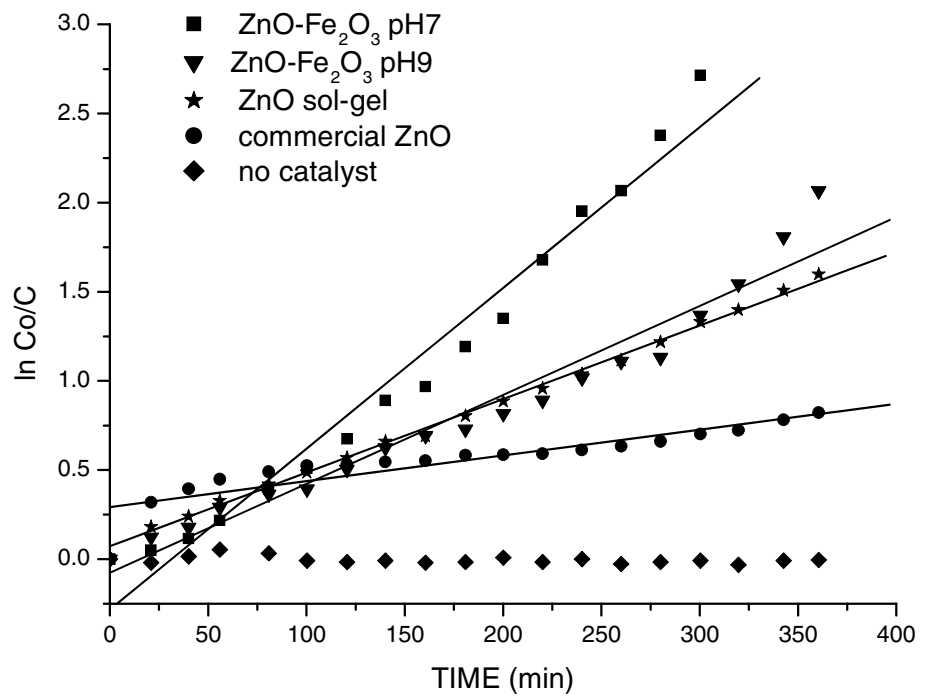


Table 2 Specific surface area values and photocatalytic activity results of ZnO-Fe₂O₃ and pure Zinc oxide catalysts

Sample	Synthesis pH	Surface area (m ² /g)	<i>K</i> (min ⁻¹)	<i>t</i> _{1/2} (min)
ZnO-Fe ₂ O ₃	7	7.2	9.7×10^{-3}	71.0
ZnO-Fe ₂ O ₃	9	4.8	4.8×10^{-3}	144.0
ZnO sol-gel	9	10.7	4.3×10^{-3}	165.0
Commercial ZnO	–	6.0	1.6×10^{-3}	433.0

Photocatalytic activity

Figure 6 shows first order reaction for cyanide decomposition. The ZnO-Fe₂O₃ sol-gel powder obtained at pH 7 exhibits much better activity than mixed oxide prepared at pH 9, indicated by high rate constant and low half time values reported in Table 2, however, both mixed oxides have better performance than sol-gel and commercial ZnO. This fact is also consequence of the hydroxyl group presence on the mixed semiconductor due to preparation method. It is known that hydroxyl groups tied at crystalline structure act as active sites [33]. On the other hand, the best activity of the mixed oxide prepared at pH 7, is attributed to the lower iron content, approximately 0.5 atomic percentages, which seems to be in the optimum content range. It was reported that higher iron content in coupling oxides causes a reduction on the distance that separates photoelectrons from photoholes, which reflects an inefficient activity of the solids on photocatalytic process [29].

Conclusions

In spite of few researches which have reported a better photocatalytic activity for pure zinc oxide than other mixed oxides, it has been demonstrated that the synthesis conditions of the coupled semiconductors cause a change on this behavior. On the other hand, the nature of the substrate to be degraded also determines the activity of the semiconductor. Hence, in this research work, under established conditions, the mixed oxide with low iron content synthesized at pH 7, shows the best activity on potassium cyanide decomposition. The organic compounds degradation with ZnO-Fe₂O₃ catalyst will be investigated in our researcher group.

Acknowledgments The authors gratefully acknowledge the financial support by grants: PROMEP/103.5/05/227 and PAICYT CA1048-05. We are grateful to Esthela Gomez for technical assistance in EDS analysis.

References

- Herrmann JM, Guillard Ch, Disdier J, Lehaut C, Malato S, Blanco J (2002) *Appl Catal B: Environ* 35:281
- Herrmann JM (1994) *Trends Photochem Photobiol* 3:633
- Fox MA, Dulay MT (1993) *Chem Rev* 93:341
- Herrmann JM (2001) *Helvetica Chimica Acta* 84:2731
- Malato S (2004) *Thessalonica*
- Valenzuela MA, Bosch P, Jimenez-Becerril J, Quiroz O, Páez AI (2002) *J Photochem Photobiol A: Chem* 148:177
- Sene Jeosadeque J, Mzeltner WA, Anderson MA (2003) *J Phys Chem B* 107:1597
- Chiang K, Amal R, Tran T (2002) *Adv Environ Res* 6:471
- Sadeghi M, Liu W, Zhang T-G, Stavropoulos P, Levy B (1996) *J Phys Chem* 100:19466
- Ho W, Yu JC, Lin J, Yu J, Li P (2004) *Langmuir* 20:5865
- Serpone N (1995) *Photochem Photobiol A: Chem* 85:247
- Villaseñor J, Reyes P, Pecchi G (1998) *J Chem Technol Biotechnol* 72:105
- Pal B, Sharon M (2002) *Mater Chem Phys* 76:82
- Marci G, Augugliaro V, López-Muñoz MJ, Martín C, Palmisano L, Rives V, Schiavello M, Tilley RJD, Venezia AM (2001) *J Phys Chem B* 105:1026
- Marci G, Augugliaro V, López-Muñoz MJ, Martín C, Palmisano L, Rives V, Schiavello M, Tilley RJD, Venezia AM (2001) *J Phys Chem B* 105:1033
- Sánchez-Mora E, Gómez-Barojas E, Gracia-Jiménez JM, Silva-González R, Pérez-Rodríguez F (2004) *Phys Stat Sol (c)* 1: s-116
- Shaogui Y, Xie Q, Xinyong L, Yazhi L, Shuo C, GuoHua C (2004) *Phys Chem Chem Phys* 6:659
- Yuan Z-H, Zhang L-D (2001) *J Mater Chem* 11:1265
- Brinker CJ, Scherer GW (1990) *Sol gel science*. Academic Press, New York
- Livage J (1986) *J Solid State Chem* 64:322
- Livage J, Henry M, Sánchez C (1988) *Prog Solid St Chem* 18: 259
- Lopez T, Sanchez E, Bosch P, Meas Y, Gomez R (1992) *Mater Chem Phys* 32:141–152
- Hernandez A, Torres-Martinez LM, Lopez T (2002) *Mater Lett* 54:62
- Nakamoto K (1978) *Infrared and raman spectra of inorganic and coordination compounds*. John Wiley & Sons
- Ferraro JR (1971) *Low frequency vibrations of inorganic and coordination compounds*. Plenum Press, New York
- Lopez T, Mendez J, Zamudio T, Villa M (1992) *Mater Chem Phys* 30:161–167
- JCPDS 36-1451, McMurdie H (1986) *Powder Diffraction* 1:76
- West AR (1992) *Solid state chemistry and its applications*. John Wiley & Sons, Great Britain
- Sakthivel S, Geissen S-U, Bahnemann DW, Murugesan V, Vogelpohi A (2002) *J Photochem Photobiol A: Chem* 148:283
- Grumes A, Leapman RD, Wilker CN, Hoffmann R, Kuns AB (1982) *Phys Rev B* 25:7157
- López T, Alvarez M, Gomez R, Aguilar DH, Quintana P (2005) *J Sol-Gel Sci Technol* 33:93
- Serpone N, Pellizetti E (1989) *Photocatalysis fundamentals and applications*. John Wiley & Sons
- Ding Z, Lu GQ, Greenfield PF (2000) *J Phys Chem B* 104: 4815